Available online at www.sciencedirect.com

SciVerse ScienceDirect

Ceramics International 39 (2013) 8049–8057

CERAMICS INTERNATIONAL

www.elsevier.com/locate/ceramint

Effect of La substitution on the structural and electrical properties of $BaBi_{4-x}La_xTi_4O_{15}$

J.D. Bobić[a,*], M.M. Vijatović Petrović[a], J. Banys[b], B.D. Stojanović[a]

[a]*Institute for Multidisciplinary Researches, Belgrade University, Kneza Viseslava 1, Belgrade, Serbia*
[b]*Faculty of Physics, Vilnius University, 9 Sauletekio, Vilnius, Lithuania*

Received 13 February 2013; received in revised form 21 March 2013; accepted 21 March 2013
Available online 4 April 2013

Abstract

Pure and lanthanum doped barium bismuth titanate $BaBi_{4-x}La_xTi_4O_{15}$ (BBLT, $x=0$, 0.05, 0.15, 0.30) ceramics were prepared utilizing solid state method. The X-ray diffraction (XRD) data confirmed formation of single-phase Aurivillius compounds while SEM micrographs did not show evident grain size change of doped ceramics. Dielectric properties were investigated in 1.21 kHz to 1 MHz frequency range and in the temperature range of 20 to 727 °C. When Bi^{3+} is substituted with La^{3+}, a significant disorder was induced and the material exhibited broadening of the phase transition. Impedance analysis confirmed the presence of two semicircular arcs in doped samples suggesting the existence of grain and grain-boundary conduction. The dc-conductivity and activation energies were evaluated for all compositions.

Keywords: A. Powders: solid state reaction; C. Dielectric properties; C. Electrical conductivity

1. Introduction

Lead-based piezoelectric relaxor ceramics, such as $Pb(Mg_{1/3}Nb_{2/3})O_3$ (PMN) or $(Pb,La)(Zr,Ti)O_3$ (PLZT), are widely used in piezoelectric actuators, sensors and transducers [1–3]. However, due to evaporation of toxic lead oxides during high-temperature sintering there is a growing need for new, ecologically clean, lead-free ceramics for various applications. Several Aurivillius compounds, like $Bi_4Ti_3O_{12}$, $SrBi_2Nb_2O_9$, $BaBi_4Ti_4O_{15}$, have properties desirable for next generation of ceramics. These materials have high Curie temperature which facilitates their wide applicability for improved performance of many electronic devices [4].

The crystal structure of bismuth-based materials is composed of $(Bi_2O_2)^{2+}$ layers interleaved with perovskite-like blocks $(A_{m-1}B_mO_{3m+1})^{2-}$, which promotes a plate-like morphology growing preferentially in the *ab* plane [5]. In comparison with almost isotropic (cubic) structure of PMN and PZT [6,7], their intrinsic electrical properties are anisotropic with the maximum value of conductivity and the major component of spontaneous polarization parallel to the $(Bi_2O_2)^{2+}$ layers [8]. One problem in application of bismuth titanate based ceramics for many devices is their high conductivity. This conductivity is an electronic p-type, where oxygen vacancies are main conduction species in bismuth layered compounds, which can be suppressed by donor doping [9–11] or grain size reducing [12,13].

Dielectric and ferroelectric properties of bismuth compounds could be controlled by substitution of ions on A and/or B sites of perovskite like slabs with ions of the proper ionic radii and valency. It is believed that the chemical stability of the perovskite layer against oxygen vacancies would be drastically improved with isovalent A-substitution of Bi^{3+} with La^{3+} ions [14–16]. There are just a few reports regarding La^{3+} substitution on Bi^{3+} positions in BBT ceramics available in the literature [17,18]. Chakrabarti and co-authors reported that incorporation of La-ions results in a significant reduction in the dc-conductivity for x=0.3 composition (according to formula $BaBi_{4-x}La_xTi_4O_{15}$) prepared by chemical method.

The purpose of this study was to investigate dielectric behavior and the mechanism of electrical transport in BBT and La substituted BBLT compounds obtained by solid state method.

*Corresponding author. Tel.: +381 11 2085 039; fax: +381 11 2085 062.
E-mail address: jelenabobic@yahoo.com (J.D. Bobić).

0272-8842/$ - see front matter © 2013 Elsevier Ltd and Techna Group S.r.l. All rights reserved.
http://dx.doi.org/10.1016/j.ceramint.2013.03.075

2. Experimental

The compositions of $BaBi_{4-x}La_xTi_4O_{15}$ (x=0, 0.05, 0.15 and 0.30 denoted as BBT, BBLT5, BBLT15 and BBLT30) were prepared via the conventional solid-state reaction method as reported elsewhere [9]. Stoichiometric amounts of high purity oxides: BaO, TiO_2, Bi_2O_3 and La_2O_3 (Alfa Aesar, p.a. 99%) were homogenized in isopropanol medium for 24 h in a planetary ball mill (Fritsch Pulverisette 5). The obtained powder was calcined at 950 °C for 4 h and pressed into pellets (49 MPa) using a uniaxial press (8 mm in diameter and ~3 mm thick). Ceramic samples were prepared by conventional sintering at 1130 °C, 1140 °C and 1150 °C depending on the composition in order to get dense ceramics. The sintering was performed in sealed alumina crucibles to avoid bismuth loss. The heating rate was 3 °C/min with natural cooling in air. The density of obtained ceramics was calculated geometrically.

The formation of phase and crystal structure of BBT ceramics were verified using a conventional X-ray diffractometer (XRD, Model D5000, Siemens). The diffraction setup detected CuK_α radiation, employing 2θ range between 10° and 70° at step size of 0.02° ($\Delta 2\theta$), with divergence slit of 0.5 mm and receiving slit of 0.3 mm. The morphology and microstructure of obtained ceramics were examined using scanning electron microscope (SEM, Model JEOL-JSM 5300 and SEM, Model TESCAN SM-300). For microstructure examination, the disc shape sintered samples were polished using silicon carbide paper to a 1 mm thickness and cleaned in an ultrasonic ethanol bath. Platinum paste was painted on both sides of ceramic pellets and fired at 750 °C to form the electrodes for electrical measurements. The dielectric constant measurements of sintered samples were performed using a HP 4284A in the 1.21 kHz to 1 MHz frequency range and temperature interval from 20 °C to 727 °C. The temperature was controlled with a programmable oven with an accuracy of 1 °C. The impedance measurements were analyzed using commercially available Z-View software.

3. Results and discussion

The crystal structure of the sintered samples (BBLT) was characterized by XRD analysis (Fig. 1). The X-ray diffraction pattern of all samples recorded using a conventional diffractometer, can be well fitted in a tetragonal structure (identified using JCPDS no. 35-0757) with non-polar space group *I*4/*mmm*. A number of authors [19,20] have also suggested the existence of tetragonal crystal structure using conventional diffractometers. Meanwhile, Kennedy and co-authors [21] have studied the structure of these Aurivillius compounds using high resolution synchrotron diffraction methods. They found out that the structure of BBT is in fact orthorhombic (with $A2_1am$ space group).

Since the radius of the trivalent La^{3+} (1.16 Å) ion is not significantly different from Bi^{3+} (1.17 Å) ion, no appreciable change of Bragg peaks was observed in the doped patterns. Thus, the X-ray Bragg peaks in all these samples could be indexed to a pure Bi-layered perovskite structure with m=4

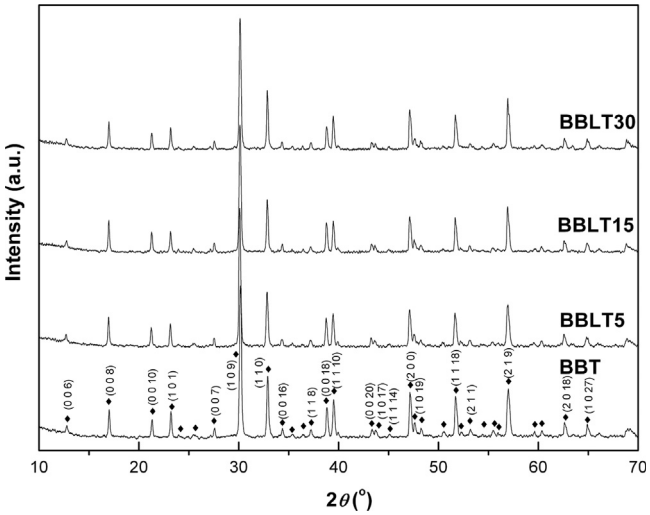

Fig. 1. X-ray diffraction patterns of the BBT, BBLT5, BBLT15 and BBLT30 ceramics.

Table 1
Influence of sintering temperature on density of BBLT ceramics.

Sample	ρ (1120 °C)%	ρ (1130 °C)%	ρ (1140 °C)	ρ (1150 °C)
BBT	79.3	88.9	melting	–
BBLT5	80.8	85.6	90.8%	melting
BBLT15	74.9	78.7	83.3%	94.3%
BBLT30	73.3	75.6	80.1%	90.0%

(number of perovskite blocks). This observation is in agreement with other studies showing complete solid solubility of lanthanum ions in the lattice of $Bi_4Ti_3O_{12}$ and $BaBi_4Ti_4O_{15}$ in the composition range $x \leq 1.0$ [16,17,22].

Table 1 illustrates the density of the samples at different sintering temperatures. The density of the samples increased with La doping till $x \leq 0.15$ concentration and then started to decrease. In the case of BBLT15 and BBLT30 higher sintering temperature (1150 °C) was needed to achieve satisfactory density.

Microstructures of four representative samples (BBT, BBLT5, BBLT15 and BBLT30) are shown in Fig. 2. The micrographs of all samples revealed plate-like grains with dimensions up to 2 μm width and 0.1 μm thickness. There is no evident change in doped ceramics grain size compared to undoped ones.

The variation of the dielectric constant (ε_r) and dielectric losses as a function of temperature at various frequencies for every sample (BBT, BBLT5, BBLT15 and BBLT30) is shown in Fig. 3. The temperature of dielectric constant maximum (T_m) of BBLT specimens significantly decreases with the increase of lanthanum content. All the lanthanum doped samples have higher values of the room temperature dielectric constant (ε_{RT}) and tan δ than that of pure BBT (Table 2). Clearly, the decline of T_m for all synthesized BBLT ceramics can be attributed to the subtle change caused by incorporating La^{3+} ions into the original BBT lattice.

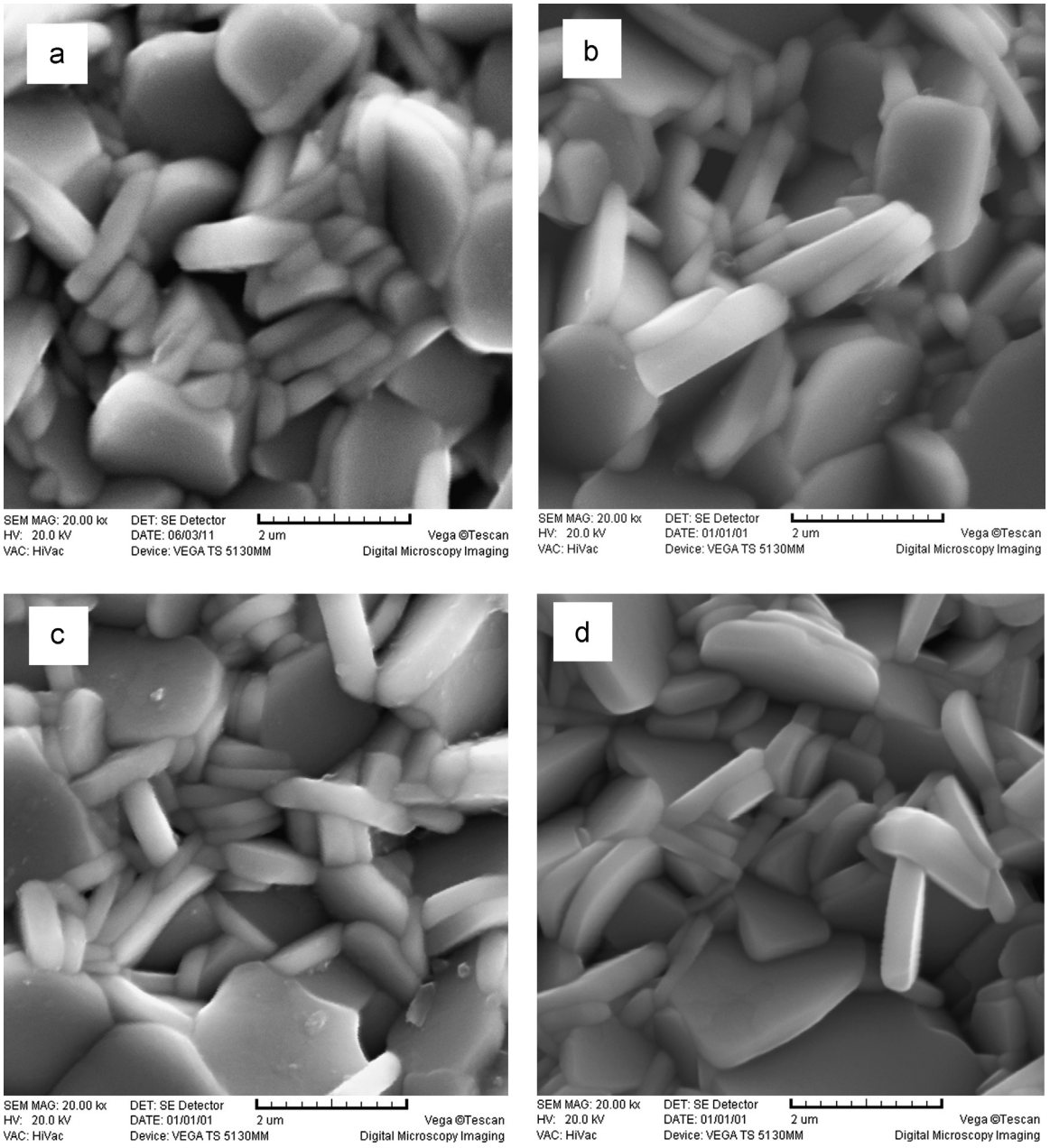

Fig. 2. SEM micrograph of sintered ceramics: (a) BBT, (b) BBLT5, (c) BBLT15 and (d) BBLT30.

Well-known modified Curie–Weiss law describes the ε' peak at high temperatures and the diffuseness of the phase transition. Parameter γ, shown in Table 2, typically indicates the degree of diffuseness of the material ($\gamma=1$ for normal ferroelectrics and $\gamma=2$ for relaxor). The numerical value of γ was determined from plot of $\ln(1/\varepsilon-1/\varepsilon_m)$ vs. $\ln(T-T_m)$. However, for $T>T_m$, γ does not reflect the exact increase of diffuseness. Thus several relations have been used to describe the dielectric permittivity of relaxor, one of which is Lorenz-type empirical relation proposed by Bokov [23]:

$$\frac{\varepsilon_A}{\varepsilon}=1+\frac{(T-T_A)^2}{2{\delta_A}^2} \quad (1)$$

where the temperature (T_A) and the magnitude (ε_A) of the Lorenz height generally differ from the T_m and ε_m of the experiments. The parameter δ, unlike γ, is frequency independent and characterizes the diffuseness of the peak. Good fits are achieved at low and high temperature part of dielectric permittivity indicating that there should be only one polarization process in all ceramics [24]. The results of fitting are shown by the solid line in Fig. 4 and in Table 2. Note that the increase of parameter δ with increase of La concentration indicates an increase of the degree of diffuseness of the dielectric peak. Lanthanum substitution induces the chemical and structural inhomogeneity, which leads to the structural short-range disorder in the lanthanum doped ceramics and thus causes diffuseness of the peak.

Detected frequency dispersion of the dielectric constant in BBT samples indicates relaxor behavior of the material. The degree of relaxation, shown in Table 2, was calculated for all

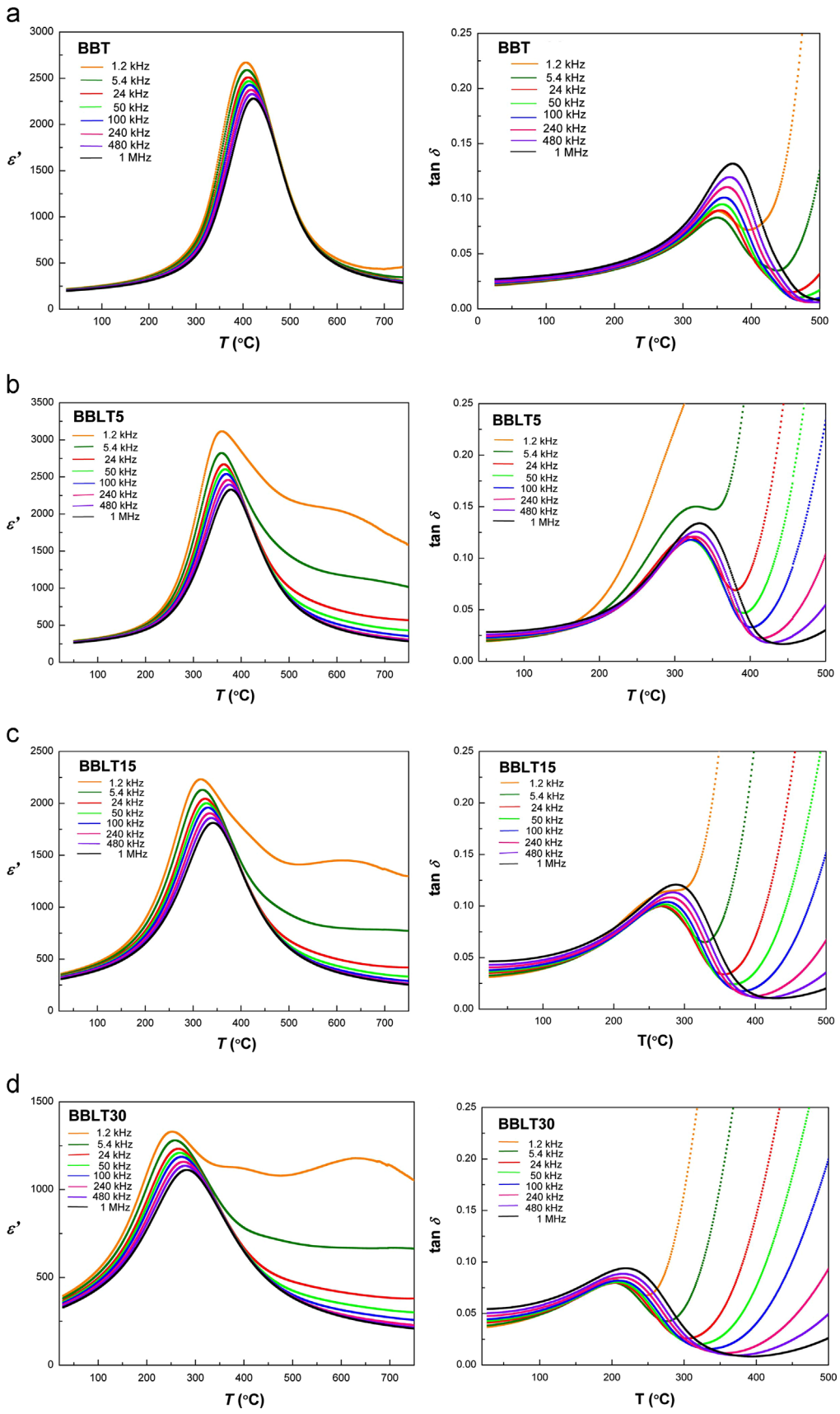

Fig. 3. The temperature dependence of dielectric constant and dielectric losses of BBLT specimens at different frequencies.

Table 2
The room temperature dielectric constant (ε_{RT}), the peak dielectric constant (ε_m), temperature of the dielectric maximum (T_m), room temperature dielectric losses (tan δ), the degree of diffuseness (γ), the degree of relaxation behavior (ΔT_{relax}), and fitting parameters (δ, ε_A, T_A) of the Lorenc type formula which are measured at 100 kHz for different compositions.

Sample	ε_{RT}	ε_m	T_m (°C)	tan δ_{RT}	γ	ΔT_{relax}	$T < T_c$			$T > T_c$		
							δ	ε_A	T_A (°C)	δ	ε_A	T_A (°C)
BBT	204	2429	415	0.024	2.05	16	46.2	2412	409	59.3	2417	418
BBLT5	273	2540	369	0.032	1.80	20	51.3	2535	368	68.4	2576	361
BBLT15	327	1959	331	0.040	1.81	26	69.6	1981	336	80.0	1978	324
BBLT30	353	1187	271	0.045	1.85	30	91.7	1200	279	108.3	1204	259

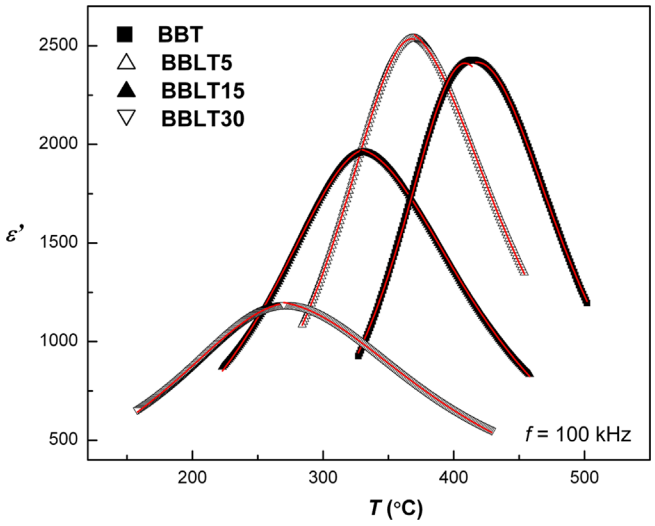

Fig. 4. Lorenz fitting of the dielectric constant of the BBT, BBLT5, BBLT15 and BBLT30 ceramics.

compositions as $\Delta T_{relaxor} = T_{m(1.21\ MHz)} - T_{m(1\ kHz)}$. The degree of relaxation of the ferroelectric–paraelectric phase transition increased with further increase of x.

In relaxor ferroelectrics the frequency dependence of the temperature of the dielectric peak is found to obey the Vogel–Fulcher law:

$$\nu = \nu_0 exp\left\{\frac{-E_a}{k_B(T_m - T_f)}\right\} \quad (2)$$

where ν_0 is the Debye frequency—the attempt frequency of dipole reorientation, E_a is the activation energy (i.e., the energy barrier between two equivalent polarization states), k_B is the Boltzmann's constant, and T_f is the static freezing temperature of the polarization fluctuations (i.e., the temperature below which dynamic reorientation of the dipolar cluster polarization can no longer be thermally activated). The temperature of the dielectric peak T_m shows a good fit to the Vogel–Fulcher law (Fig. 5), showing typical relaxor behavior. The values for the fitting parameters are listed in Table 3. The E_a increases with increase in La^{3+} concentration confirming strengthening in the relaxor behavior. The same trend was observed in the work of Chakrabarti and co-authors [17]. Attempt frequency of the ions in the solid state is in the order of only 10^{12}–10^{13} Hz [25]. It was also found that attempt frequency increases with the increase in La content, but for BBLT15 and BBLT30 it was higher than the upper limit of its physical meaning. It was suggested that there are different types of relaxation occurring in these two compositional regions [26].

The ac conductivity (σ_{AC}) of the BBLT ceramic materials at different temperatures was calculated using the relation $\sigma_{AC} = \varepsilon_0 \varepsilon_r \tan\delta$, where the symbols have their usual meanings. The frequency dependence of σ_{AC} of the materials in temperature range of 327 °C to 727 °C is shown in Fig. 6. Two different conductivity regions of undoped BBT samples are distinguishable in the experimental frequency range. A frequency independent plateau in conductivity spectra can be seen in the low frequency range and can be explained by jump relaxation model [27]. Apart from frequency independent plateau, one more dispersion region appears in the conductivity spectra associated with the grain. For doped samples, besides the existing, the third dispersion region appear in the conductivity spectra indicating the enhancement of mobile charge carriers through the grain boundary. This will be supported by the conclusion drawn from complex impedance spectra.

DC conductivity data can be theoretically predicted from extrapolation of ac-conductivity data on y-axis from σ_{AC} vs. frequency (Fig. 6). The obtained values of σ_{DC} at different temperatures enable determination of the activation energy for conduction process (E_{DC}) according to the Arhenius law: $\sigma_{DC} = \sigma_0 \exp(-E_{DC}/kT)$. This is graphically presented in Fig. 7 as $\ln(\sigma_{DC})$ vs. $1000/T$. Activation energies for BBT, BBLT5, BBLT15 and BBLT30 ceramics were 0.89 eV, 0.67 eV, 0.69 eV and 0.76 eV respectively, where E_{DC} values reflect the measured total conductivity. All the lanthanum doped samples have lower activation energies in comparison to pure BBT. The E_{DC} decrease with addition of the minimum concentration of La, while with further increase of the La content the value of E_{DC} increases. The value of activation energies for conduction clearly suggested a possibility that the conduction in the high temperature range was ionic due to oxygen vacancies resulted from Bi volatilization according to Eq. (3) [28]:

$$Bi_2O_3 = 2\,Bi + 3/2O_2\uparrow + 2V''_{Bi} + 3V_O \quad (3)$$

At first La introduces a certain quantity of oxygen vacancies in BBT ceramics increasing the conductivity of pure BBT. After that, with higher concentration of La ($x > 0.05$) conductivity starts to decrease (Fig. 8). This could be explained by

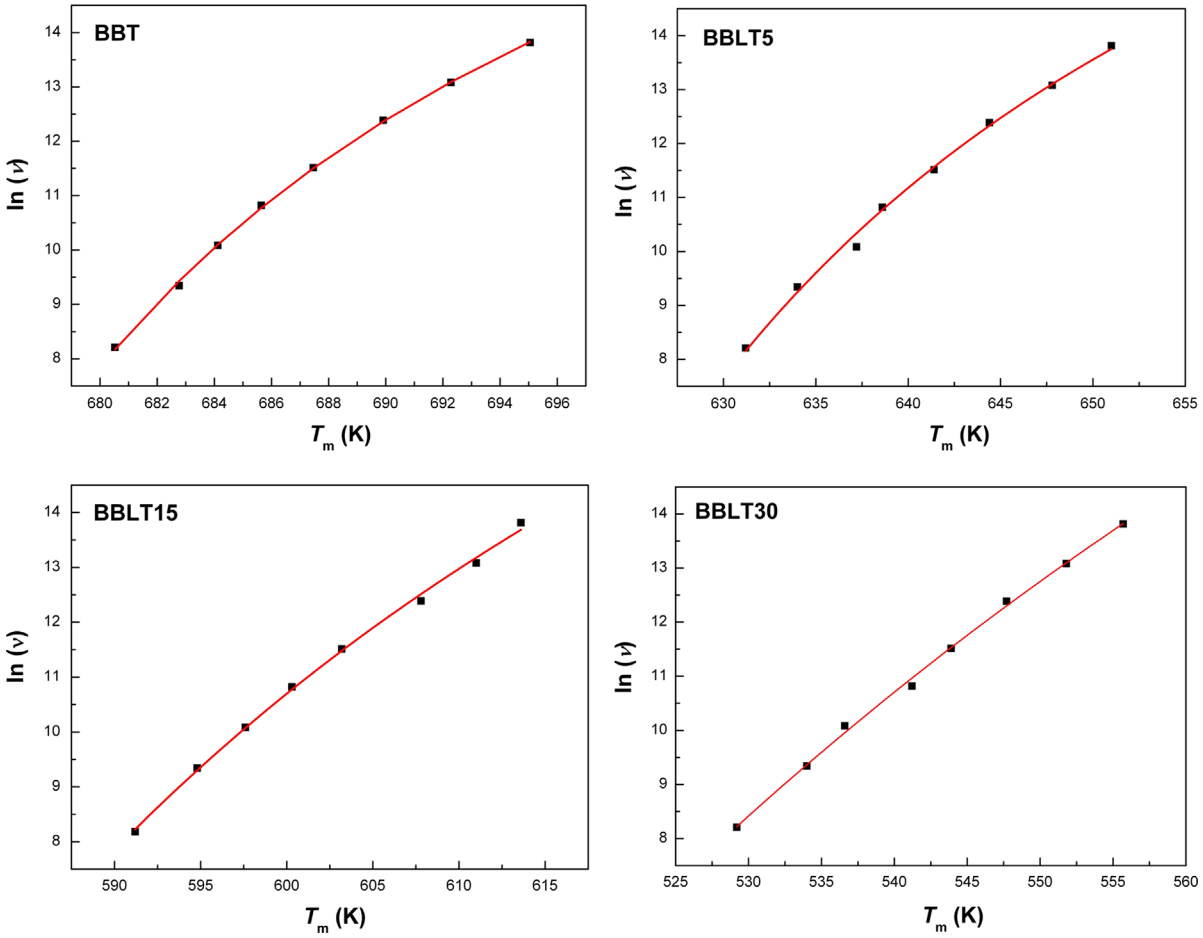

Fig. 5. Temperature of the dielectric maximum T_m as a function of ln(ν) for the BBT ceramics (the square dots represent the experimental data and the solid line is the fit to the Vogel–Fulcher relation).

Table 3
Fitting parameters ($E_{a,VF}$, T_f, v_0) of the Vogel–Fulcher relation measured at 100 kHz and activation energy E_{DC} according to the Arrhenius law.

Sample	Vogel–Fulcher parameters		
	E_a (eV)	v_0 (Hz)	T_f (K/°C)
BBT	0.034	1.85 × 1010	654/381
BBLT5	0.064	1.42 × 1011	589/316
BBLT15	0.174	2.94 × 1014	511/238
BBLT30	0.595	2.65 × 1021	361/88

the fact that further La substitution supresses the volatility of Bi and then decreases concentration of oxygen and bismuth vacancies [29,14].

Complex impedance spectrum was obtained from the variation of real $Z' = \varepsilon''/2\pi f\varepsilon_0(\varepsilon''^2 + \varepsilon'^2)$ and imaginary part $Z'' = \varepsilon'/2\pi f\varepsilon_0(\varepsilon''^2 + \varepsilon'^2)$ of impedance (Fig. 9). This was used to separate the grain and grain boundary effects due to their different relaxation frequencies of the relaxation processes in the grain and grain boundaries. In the present investigation, only a single semicircle is observed in the 850–1000 K (577 °C–727 °C) temperature range in undoped BBT ceramic. Therefore, it is reasonable to ascribe this semicircle to the grain component. In doped BBLT ceramics two semicircles could be traced. The intercepts of the high frequency and low frequency arcs give the grain resistance (R_g) and grain-boundary resistance (R_{gb}), respectively. As it was presented in Fig. 9 and from the value of conductivity (Table 4), the total or dc conductivity of doped samples are fully controlled by the conductivity of the grain at temperatures above 850 K (in a serial model the lower conductive element of the circuit controls and limits the total dc conductivity of the system [30]). At elevated temperatures charge carrier of oxygen vacancies can easily migrate and accumulate at grain boundaries and thus enhance the conduction of grain boundaries. The grain conductivity, being lower than grain boundary one, controls the material conductivity.

4. Summary

In summary, utilizing the method of solid-state reaction, the dense ceramics of La-doped $BaBi_4Ti_4O_{15}$ were prepared. According to SEM micrographs, there is no evident change of grain size in doped ceramics compared to undoped ones.

A relaxor-type dielectric permittivity peak was observed in all samples. This was confirmed by increase of the degree of relaxation from 16 for undoped BBT to 30 for x=0.30

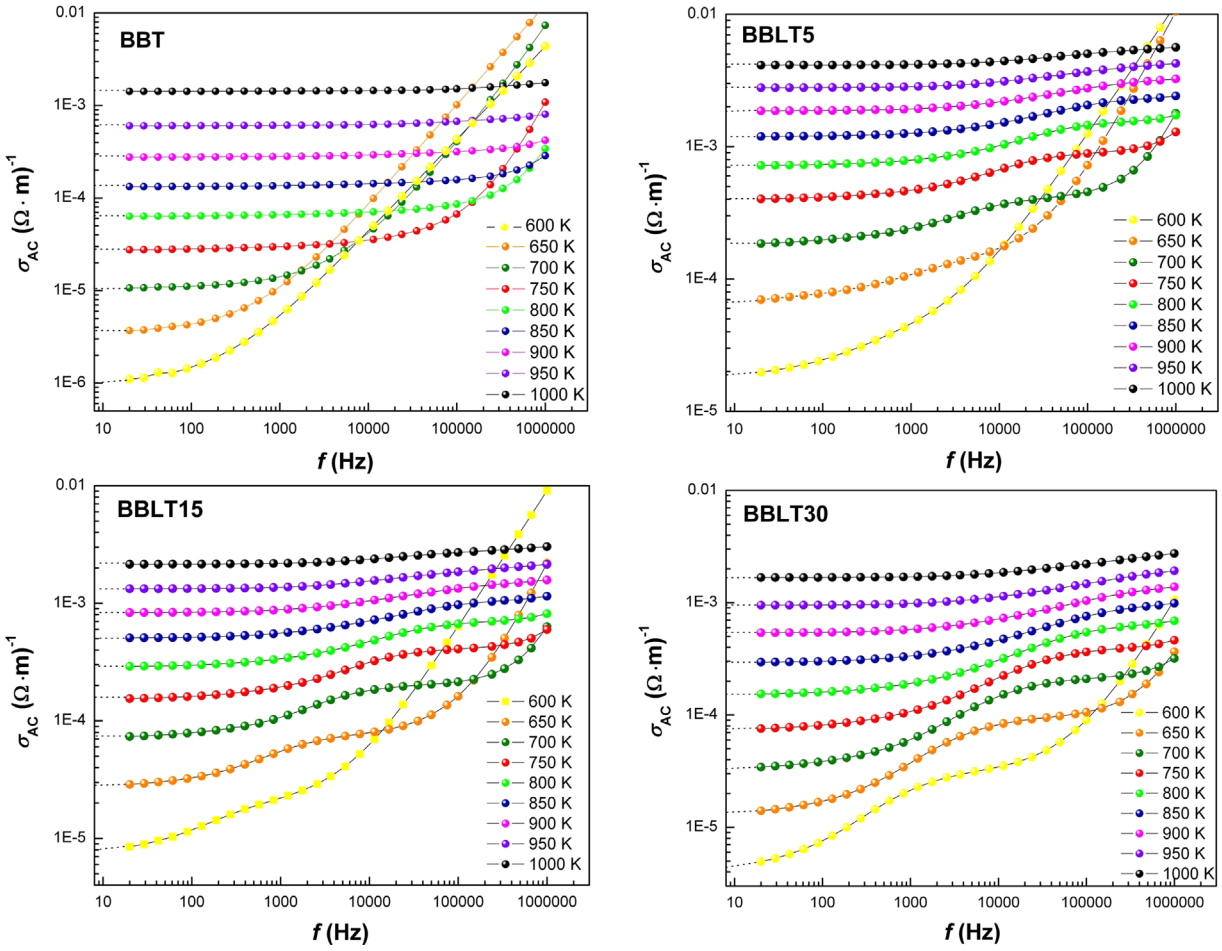

Fig. 6. Variation of ac conductivity with frequency at different temperatures for BBLT compounds.

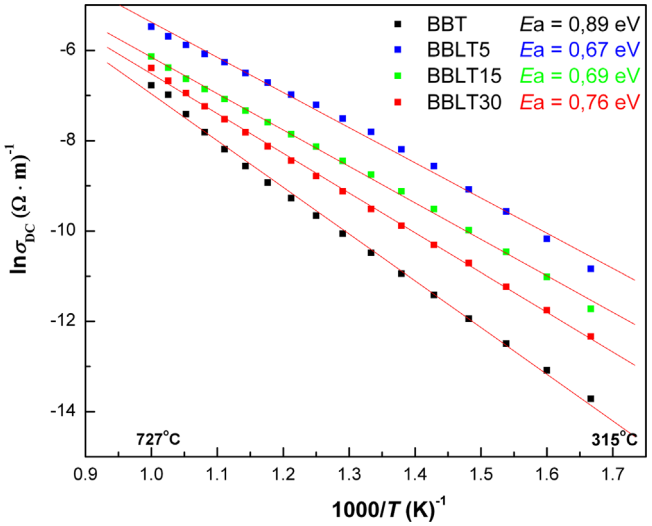

Fig. 7. Arrhenius plots of dc conductivity of BBT, BBLT5, BBLT15 and BBLT30 ceramics.

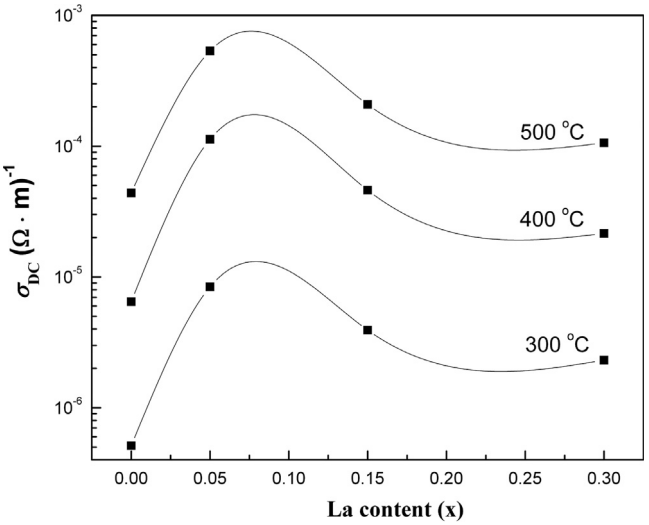

Fig. 8. Variation of the dc conductivity as a function of the La doping at three different temperatures.

La-doped sample. The diffuseness also increased with the increase of La concentration.

The incorporation of La^{3+} resulted at first in a conductivity enhancement for lower concentration of La ($x \leq 0.05$) but then it decreased with the increase in the La content. This could be explained by the fact that further La substitution supresses the volatility of Bi and then decreases the concentration of oxygen and bismuth vacancies.

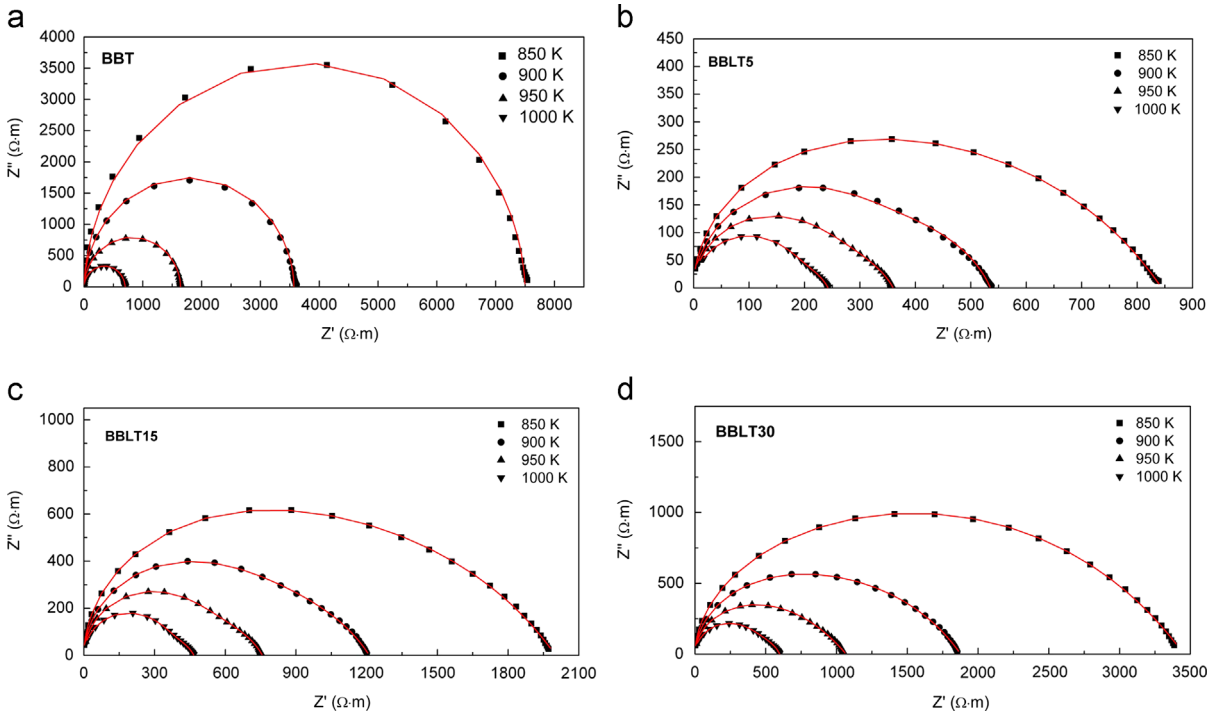

Fig. 9. Complex impedance plot of the BBLT ceramics at different temperatures.

Table 4
Dc conductivity for grain and grain boundary at different temperatures for all compositions.

Temp. (K)	**BBT**	**BBLT5**		**BBLT15**		**BBLT30**	
	σ_g (Ω m)$^{-1}$	σ_g (Ω m)$^{-1}$	σ_{gb} (Ω m)$^{-1}$	σ_g (Ω m)$^{-1}$	σ_{gb} (Ω m)$^{-1}$	σ_g (Ω m)$^{-1}$	σ_{gb} (Ω m)$^{-1}$
850	1.33 × 10−4	2.70 × 10−3	2.10 × 10−3	1.13 × 10−3	8.90 × 10−4	1.06 × 10−3	3.98 × 10−4
950	6.01 × 10−4	3.99 × 10−3	9.09 × 10−3	1.91 × 10−3	4.26 × 10−3	1.78 × 10−3	2.00 × 10−3
1000	1.43 × 10−3	5.81 × 10−3	1.30 × 10−2	2.79 × 10−3	9.16 × 10−3	2.62 × 10−3	4.48 × 10−3

Impedance analysis confirmed the presence of grain and grain boundary microstructural element contributions to the bulk impedance. Variation of grain and grain boundary conductivity with temperature reflects the fact that the conduction in BBLT is through grain boudary rather than grains at temperature above 850 K. At elevated temperatures charge carrier of oxygen vacancies can easily migrate and accumulate at grain boundaries and thus enhance the conduction of grain boundaries.

Acknowledgments

The authors gratefully acknowledge the Ministry of Education and Science of Republic of Serbia for the financial support of this work (project III 45021) and COST MP 0904.

References

[1] A.P. Barranco, J.D.S. Guerra, R.L. Noda, E.B. Araujo, Ionized oxygen vacancy-related electrical conductiviry in $(Pb_{1-x}La_x)(Zr_{0.90}Ti_{0.10})_{1-x/4}O_3$ ceramics, Journal of Physics D: Applied Physics 41 (2008) 215503–215508.

[2] G.H. Heartling, C.E. Land, Hot-pressed (Pb,La)(Zr,Ti)O_3 ferroelectric ceramics for electro-optic applications, Journal of the American Ceramic Society 54 (1971) 1–10.

[3] V.V. Shvartsman, D.C. Lupascu, Lead-free relaxor ferroelectrics, Journal of the American Ceramic Society 95 (1) (2012) 1–26.

[4] A.Q. Jiang, Z.X. Hu, L.D. Zhang, The induced phase transformation and oxygen vacancy relaxation in La-modified bismuth titanate ceramics, Applied Physics Letters 74 (1) (1999) 114–116.

[5] B. Aurivillius, Mixed bismuth oxides with layer lattices, III structure of $BaBi_4Ti_4O_{15}$, Arkiv för Kemi 1 (1950) 519–527.

[6] A.J. Paulaa, A.A. Cavalheirob, J.C. Brunob, M.A. Zaghetea, Elson Longoa, J.A. Varela, A homovalent doping in PMN ceramics by using lithium and scandium cations, Materials Chemistry and Physics 112 (2008) 886–891.

[7] B.W. Lee, E.J. Lee, Effects of complex doping on microstructural and electrical properties of PZT ceramics, Journal of Electroceramics 17 (2006) 597–602.

[8] D. Damjanovic, Hysteresis in piezoelectric and ferroelectric materials, in: I. Mayergouz, G. Bertotti (Eds.), The Science of Hysteresis, vol. 3, Elsevier, Oxford, UK, 2005.

[9] J.D. Bobić, M.M. Vijatović Petrovića, J. Banys, B.D. Stojanovića, Electrical properties of niobium doped barium bismuth–titanate ceramics, Materials Research Bulletin 47 (2012) 1874–1880.

[10] L. Zhang, R. Chu, S. Zhao, G. Li, Q. Yin, Microstructure and electrical properties of niobium doped $Bi_4Ti_3O_{12}$ layer-structured piezoelectric ceramics, Materials Science and Engineering B 116 (2005) 99–103.

[11] H.S. Shulman, D. Damjanović, N. Setter, Niobium doping and dielectric anomalies in bismuth titanate, Journal of the American Ceramic Society 83 (3) (2000) 528–532.
[12] M. Villegas, A.C. Caballero, C. Moure, P. Duran, J.F. Fernandez, Factor affecting the electrical conductivity of donor-doped $Bi_4Ti_3O_{12}$ piezoelectric ceramics, Journal of the American Ceramic Society 89 (9) (1999) 2411–2416.
[13] T. Jardiel, A.C. Caballero, M. Villegas, Aurivillius ceramics, $Bi_4Ti_3O_{12}$-based piezoelectrics, Journal of the Ceramic Society of Japan 116 (2008) 511–518.
[14] A.Z. Simoes, C. Quinelato, A. Ries, B.D. Stojanovic, E. Longo, J.A. Varela, Preparation of lanthanum doped $Bi_4Ti_4O_{12}$ ceramics by the polymeric precursors method, Materials Chemistry and Physics 98 (2006) 481–485.
[15] M. Osada, M. Tada, M. Kakihana, T. Watanabe, H. Funakubo, Cation distribution and structural instability in $Bi_{4-x}La_xTi_3O_{12}$, Japanese Journal of Applied Physics 40 (2001) 5572–5575.
[16] X.B. Chen, R. Hui, J. Zhu, W.P. Lu, X.Y. Mao, Relaxor properties of lanthanum-doped bismuth layer-structured ferroelectrics, Journal of Applied Physics 96 (10) (2004) 5697–5700.
[17] A. Chakrabarti, J. Bera, Effect of La-substitution on the structure and dielectric properties of $BaBi_4Ti_4O_{15}$ ceramics, Journal of Alloys and Compounds 505 (2010) 668–674.
[18] P. Fang, H. Fan, J. Li, L. Chen, F. Liang, The microstructure and dielectric relaxor behavior of $BaBi_{4-x}La_xTi_4O_{15}$ ferroelectric ceramics, Journal of Alloys and Compounds 497 (2010) 416–419.
[19] G. Nalini, T.N. Guru Row, Structure determination at room temperature and phase transition studies above T_c in A $Bi_4Ti_4O_{15}$, (A=Ba, Sr or Pb), Bulletin of Materials Science 25 (2002) 275–281.
[20] H. Irie, M. Miyayama, T. Kudo, Structure dependence of ferroelectric properties of bismuth layer-structured ferroelectric single crystals, Journal of Applied Physics 90 (8) (2001) 4089–4094.
[21] B.J. Kennedy, Y. Kubota, B.A. Hunter, Ismunandar, K. Kato, Structural phase transition in the layered bismuth oxide $BaBi_4Ti_4O_{15}$, Solid State Communications 126 (2003) 653–658.
[22] N. Pavlović, V. Koval, J. Dusza, V.V. Srdić, Effect of Ce and La substitution on dielectric properties of bismuth titanate ceramics, Ceramics International 37 (2011) 487–492.
[23] A.A. Bokov, Z.-G. Ye, Recent progress in relaxor ferroelectrics with perovskite structure, Journal of Materials Science 41 (2006) 31–52.
[24] F. HuiQing, K. ShanMing, Relaxor behavior and electrical properties of high dielectric constant materials, Science in China Series E Technological Sciences 52 (8) (2009) 2180–2185.
[25] H. Fan, J. Chen, Dielectric behavior and phase transition of perovskite PMN-PT films, Physica Scripta T139 (2010) 014039–014044.
[26] L. Wu, X. Wang, J.H. Wang, R. Guo, A.S. Bhalla, Relaxor behavior of $(1-x)BaTiO_3$–$x(Bi_{3/4}Na_{1/4})(Mg_{1/4}Ti_{3/4}O_3$ $(0.2\leq x\leq 0.9)$ ferroelectric ceramic, Journal of Materials Science 44 (2009) 5420–5427.
[27] S. Kumar, K.B.R. Varma, Dielectric relaxation in bismuth layer-srtuctured $BaBi_4Ti_4O_{15}$ ferroelectric ceramics, Current Applied Physics 11 (2011) 203–210.
[28] F.A. Kroger, H.J. Vink, Relations between the concentrations of imperfections in solids, Journal of Physics and Chemistry of Solids 5 (3) (1958) 208–223.
[29] Y.Y. Yao, C.H. Song, P. Bao, D. Su, X.M. Lu, J.S. Zhu, Y.N. Wang, Doping effect on the dielectric property in bismuth titanate, Journal of Applied Physics 95 (2004) 3126–3130.
[30] P. Duran-Martin, C. Voisard, D. Damjanović, N. Setter, Study and control of the conductivity of Nb-doped $Bi_4Ti_3O_{12}$ for high temperature piezoelectric applications, Boletin de la Sociedad Espanola de Ceramica y Vidrio 36 (6) (1999) 582–586.